The Seventh International Conference on Cold Fusion. 1998. Vancouver, Canada:, ENECO, Inc., Salt Lake City, UT. : p. 15.

MATERIAL BEHAVIOR OF HIGHLY DEUTERATED PALLADIUM

N. Asami, T. Senjuh, T. Uehara, M. Sumi, H. Kamimura, S. Miyashita and K. Matsui R&D Center for New Hydrogen Energy, The Institute of Applied Energy 14-2, Nishishinbashi 1-chome, Minato-ku, Tokyo 105, Japan

Abstract

We have presumed that achieving high reproducibility of the anomalous effect may depend upon reproducible high loading ratios of deuterium in the Palladium. By modification of the working process, heat treatment, surface treatment, and the electrolysis conditions, the deuterium loading up to 0.9~0.96 was achieved with relatively high reproducibility. Detail features of the loading and deloading process were observed by gas chromatographic (GC) analysis and by in-situ optical micrographs during electrolysis. Crystal phase and lattice parameter changes were also measured to find any new phase by the in-situ X-ray diffraction system which was newly developed at the NHE-Lab. The phase transition of $\alpha-\beta$ during the loading and unloading process was well identified, however no new phase was observed up to a loading ratio of about 0.90.

Introduction

It has been proposed that the reproducibility of the NHE phenomena is dependent mainly upon achieving control of the cathode material properties as well as the electrolysis environment. Several observers have pointed out that attaining a deuterium loading ratio greater than ~0.85 might be a prerequisite for observing the excess heat generation phenomena Material developments and analyses of cathode materials in this project has proceeded according to these postulate [l], [2], [3]. Numerous observations of the microstructures of palladium during deuterium loading and deloading has been carried out to determine the conditions for high loading. To clarify relationships between the loading characteristics and the defects formation, studies on the unelasticity of deuterated palladium were performed on various sources of palladium including pure polycrystals, single crystals, and alloys. Many kinds of crystal defects such as slip bands, micro-cracks, blistering, dislocations, etc. were observed [1], [4].

Our objectives for material development are, 1) to modify the material processing and treatment to attain high loading, 2) to find the suitable electrolysis conditions, and 3) to study the loading and deloading mechanism. For these purposes, the following experimental technologies, namely, 1) Deuterium loading experiment using electrical resistance measurement cells and GC analysis, 2) In-situ observation of the Pd surface during electrolysis, and 3) In-situ X-ray diffraction experiment, have been developed and The investigated loading characteristics of deuterated palladium will be summarized and discussed.

1. Deuterium Loading Experiments

1-1) Dependent on Pd Purity and Processing

The objectives of this development are material improvement by grain size control, purity control and surface treatment. Grain size control is generally available to introduce forging and homogenizing process during reduction of area process. Table-1 shows a example of the working procedure of 4-nine Pd material which we actually applied to manufacturing process. Grain sizes depend on the temperature of the final heat treatment process. In the case of 4-nine material, homogeneous small size grains (<100 μm) are formed at 650ºC, middle size grains (~200 μm) at 1000ºC, and large size grains(>200 μm) at 1100ºC, by heating each sample for 1 hr in a high vacuum

condition. The microstructures of grain controlled Pd of medium size grains are shown in Photo-1 for 3-nine and 4-nine Pd.

Fig. l shows the resistance change with the deuterium loading cycles stages for 4-nine Pd. Obviously, it can be found the some differences depending on the grain sizes. Fig.2 is the case of 3-nine Pd. The differences in the attained loading ratio are less than 4-nine Pd cases.

Conclusions of Item 1-1)

Conclusions of Item 1-1)

a. The forging and annealing processes are effective in attaining uniform grain size Pd Material.
b. Grain size is easier to control for purity of 3-nine than 4-nine Pd
c. Final maximum attained loading ratios (~0.96 by R/Ro with SRI scale) is similar for both 4-nine and 3-nine.
d. The smaller the grain size is for 4-nine Pd, the larger loading is attained, but no clear effect is seen for 3-nine Pd

1-2) Effect of heat treatment, surface treatment and electrolysis conditions.

The objectives of these experiments are; (1) to optimize heat treatment temperature and treatment method and, (2) to optimize electrolysis cycles. Fig.3 shows the effect of surface treatments in the case of 4 nine Pd , such as buff polish, etching by aqua-regia, etc. Fig.4 figures show the relation between attained D/Pd ratios and final heat treatment temperatures for the 2nd and 3rd electrolysis steps of pre-etched Pd.

Conclusions of Item 1-2)

a. High vacuum annealing at 900~1000ºC is suitable for attaining high loading.
b. Pre-etching with aqua-regia for short time (<10min.) is effective for removing surface impurities.
c. Step up current cycles up to 3 stages are effective, 1st stage only is not enough to attain high loading.
d. Anodic treatment between each cycles is also effective for higher loading.

2. Behavior during deuterium loading as observed by gas chromatography

The objectives of these experiments are to clarify the behavior of deuterium loading during temperature change, to determine the temperature coefficient of the Pd-D system and to investigate the correlation between R/RO and GC method for D/Pd determination. Fig.5 shows the schematic diagram of loading experiments using SRI type cells. The loading ratio is measured by the R/Ro method and by the integration of the oxygen concentration of the sampled gas. Fig.6 shows the results of loading experiments.

Generation of excess oxygen correspond to loading, and the generation of hydrogen correspond to the

deloading of deuterium. Anodic treatment is applied to each stage of electrolysis cycle. During anodic treatments, hydrogen is generated. Loading and deloading behaviors are well illustrated by this figure. Fig.7 shows the effect of the electrolyte temperature on loading. The loading ratio decreases with temperature. The loading ratio is unstable at higher temperature, near ~80ºC. The decrease in the rate of loading is about 0.002/ºC.

Conclusions of Item 2

a. Loading ratio measured by GC analysis agreed well with those measured by R/Ro method.
b. Detail structure of loading and deloading behavior are observable by GC analysis.
c. The loading ratio of Pd decreased with the rise of temperature, & increased with drop of temperature.
d. Despite heat input at high loading state (>0.95), loading ratio decreased.

3. High pressure and high temperature gas loading (HT/HP loading)

High pressure and high temperature gas loading was investigated as a means to reduce lattice defects formation and to attain high loading by subsequent electrolysis. This method was originally proposed by Dr.Violante et al. of ENEA. Designed allowable pressure and temperature of the HT/HP furnace are 50 atms, and 400°C, respectively. Deuterium loading path is performed through without the $\alpha+\beta$ two phase region in the Pd/D_2 isotherms diagram. After this gas loading, the loading ratio is measured by the weighing method. Attained loading ratios by HT/HP gas loading are about 0.65~0.68. Fig.8 shows the loading curve for both pre-loading by the HP/HT method and by electrochemical loading only. The loading features are very similar in both cases up to 4^{th} stage of the loading cycle stages. The higher loading stage, of the HT/HP pre-loading specimen shows slightly better features. Fig.9 shows a excess heat measurement using SRI type flow calorimetry system with HT/HP pre-loading specimen. No excess heat was observed.

Conclusions of Item 3

a. The loading ratios (D/Pd) which were loaded in HT/HP D_2 gas are approximately 0.65~68.
b. Even after electrolysis of these specimens, they keep their straight shape and surface smoothness.
c. D-loading behavior and attained maximum loading ratio (0.94~0.96), however, were similar to that of ordinary well controlled electrolysis (no previous gas loading treatment) cases.

4. In-situ observation of the Pd during electrolysis

The In-situ observation of the Pd during electrolysis was to observe the Pd surface phenomena during electrolysis, such as phase growth, D_2 bubble formation and absorption, and slip band or other defect formations. It can be seen the β-phase as it nucleates and grows on the inter-granular surface by the photo-2. taken after the start of electrolysis. After 5 hours, most of the surface is occupied by the β-phase, and many slip bands are observable. At this stage of loading, the averaged loading ratio is about 0.18.

Conclusions of Item 4

a. β phase nucleates and grows at intergranular surface crystal grains during the initial

stage of loading.

b. After most of the surface of bulk Pd changes to β phase, then propagates to the inside of rod.
c. Grain boundaries may act as diffusion paths for hydrogen entry into bulk of Pd.
d. Slip bands of the surface are formed during β phase growth as a result of stress release mechanism. Therefore, slip bands are able to form at relatively initial stage of loading by electrolysis.

5. In-situ X-ray diffraction experiments

In-situ X-ray diffraction experiments have been conducted to observe crystal changes during electrolysis. Fig. 10 shows the schematic figure of the X-ray diffraction measurement system. X-ray is Mo-K $_{a}$ spectrum to attain intense X-ray beams. The cross sectional view of cell arrangement is also shown in this figure. The closed cell with 9 atms, to avoid large bubble growth, and with a catalyst for recombination and with a Be window for X-ray transmission was used. Fig.11 figures show examples of diffraction pattern of deuterated specimen before and after the start of electrolysis. It can be easily seen that the Pd peaks decrease and at the same time PdD peaks grow during electrolysis.

Fig. 12 shows the results of x-ray diffraction measurements. The top figure shows the loading curve and the applied current density. The 3rd figure shows the lattice constant change of the β-phase with the loading ratio. It is very interesting that the lattice parameter of β-phase remains constant with loading up to D/Pd 0.5, and then increases linearly with loading. Fig. 13a and Fig. 13b show the diffraction patterns of β-phase PdD peaks at 0.59 and 0.91 of loading ratio respectively. No new phase (γ ?) could be found up to loading ratios of 0.91.

Conclusions of Item 5

a. Direct observation method of crystal structure by X-ray diffraction during electrolysis was developed.
b. The β phase growth and a phase decrement during electrolysis are clearly observed.
c. Lattice constant of PdD is almost constant up to a D/Pd ratio of 0.5, and linear increase of lattice constant of β phase is observed for loading ratio over 0.5.
d. No new phase appearance was observed up to a loading ratio of 0.91 during electrolysis.

References

[1] N. Asami, T. Senjuh, H. Kamimura, M. Sumi, E. Kennel, T. Sakai, K. Mori, H. Watanabe, and K.Matsui., J. of Alloys and Compounds, 253-254 (1997) 185-190

[2] T. Senjuh, H. Kamimura, T. Uehara, M. Sumi, S. Miyashita, T. Shigemitsu, and N. Asami., J. of Alloys and Compounds, 253-254 (1997) 617-620

[3] N. Hasegawa, M. Sumi, M. Takahashi, T. Senjuh, N. Asami, T. Sakai, T. Shigemitsu., Proceedings of the ICCF-5. Monte Carlo Monaco (1995) p449

[4] N. Asami, T. Senjuh, H. Kamimura, M. Sumi, E. Kennel, T. Sakai, K. Mori, H. Watanabe, and K. Matsui., Proceedings of the ICCF-6. -Progress in New Hydrogen Energy- Toya, Hokkaido, Japan Oct. 13-18 (1996) p67

Acknowledgments

The New Hydrogen Energy Project has been supported under the direction of New Energy and Industrial Technology Development Organization (NEDO). The authors are indebted to Prof. Okamoto, Prof. Ikegami, Prof. Masumoto, Prof. Sudo and all of the NHE-committee members for their guidance and valuable advice in promoting the material R&D. We would like to thank all member of NHE-Center and Laboratory, and foreign institutes especially SRI-International and INFN for their continuous collaboration.

Process	Form
Raw material	Purity of Pd: 99.99%up
Casting and melting in vacuum	30 □ m
Machining	30 □ mm → 27 □ m
Forging 900 ℃ × 1h in air	27 □ mm → 23 mm
Working	23 □ mm → 15 mm
Homogenizin	Annealed in Vac. at 850 ℃ fo 1h
Working	15 ϕ mm → 7.0 m
Homogenizin	Annealed in Vac. at 650 ℃ fo 1h
Working	7.0 ϕ mm→4.0 ϕ mm(67%)
Homogenizin	Annealed in Vac. at 650 ℃ fo 1h
Working	4.0 ϕ mm→2.0 ϕ mm(75%)
Polishin	
Cutting	Size 50 mm length
Homogenizin	Annealed in Vac. at 600 ℃ fo 1h

Modification of Grain size ~~all process and followin

Small grain size: 650 ℃ 1h in Vac. (working about 70%)

Middle grain size: 1000 ℃ 1h in Vac. (working about 30%)

Big grain size: 1100 ℃ 1h in Vac. (working about 9%)

Table-1 Working process for homogenizing 4-nine Pd

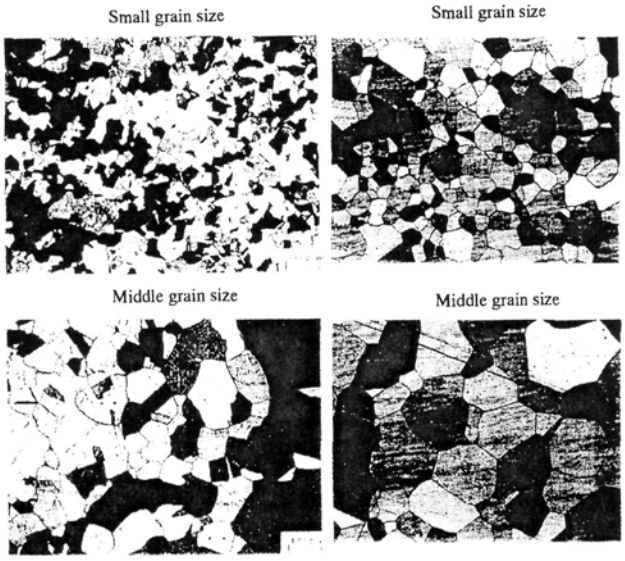

Photo-1 Microstructures of grain controlled Pd

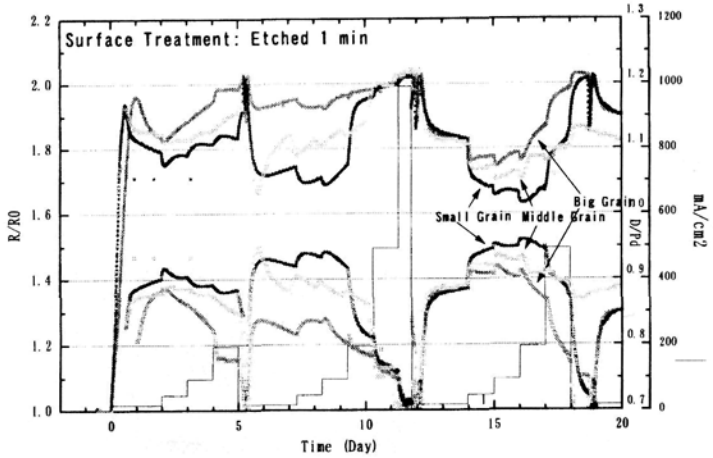

Fig.1 R/R0(upper) and D/Pd ratio(lower) changes with the d-loading cycles stages of 4-nine Pd

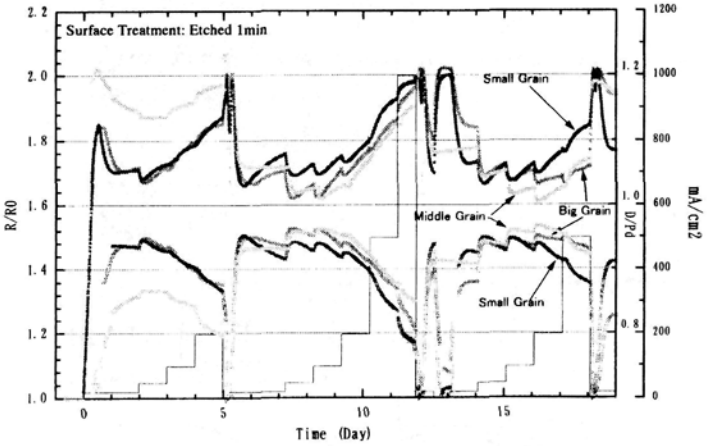

Fig.2 R/R0(upper) and D/Pd ratio(lower) changes with the d-loading cycles stages of 3-nine Pd

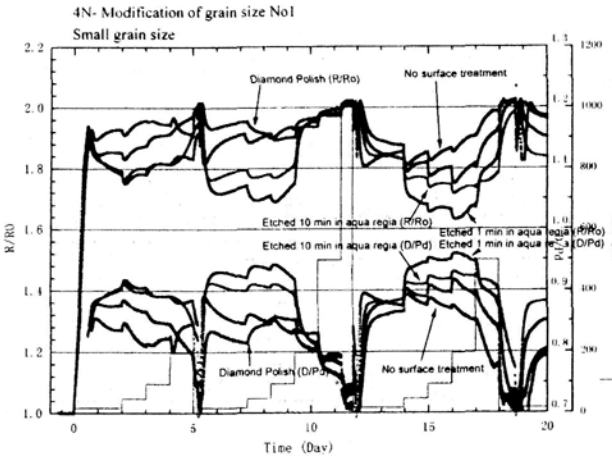

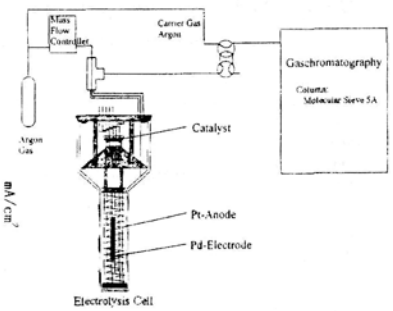

Fig. 5 Schematic diagram of GC analysis

Fig.3 Effect of surface treatments on the d-loading

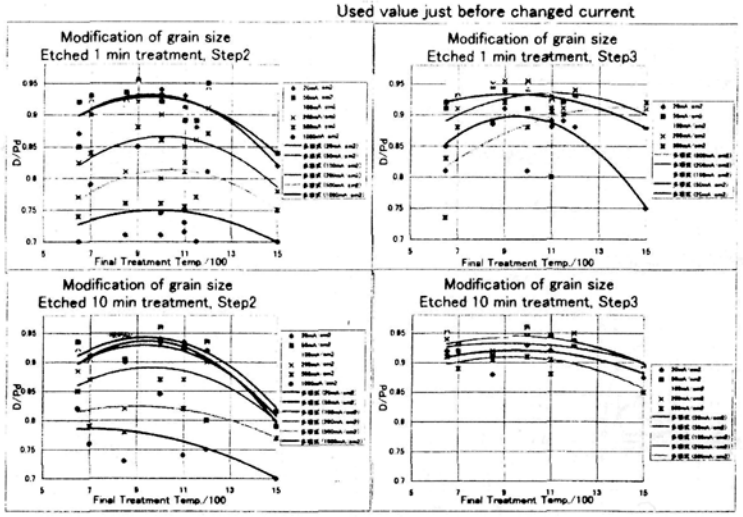

Fig.4 Relation among D/Pd ratio, final heat treatment temperatures and loading stages

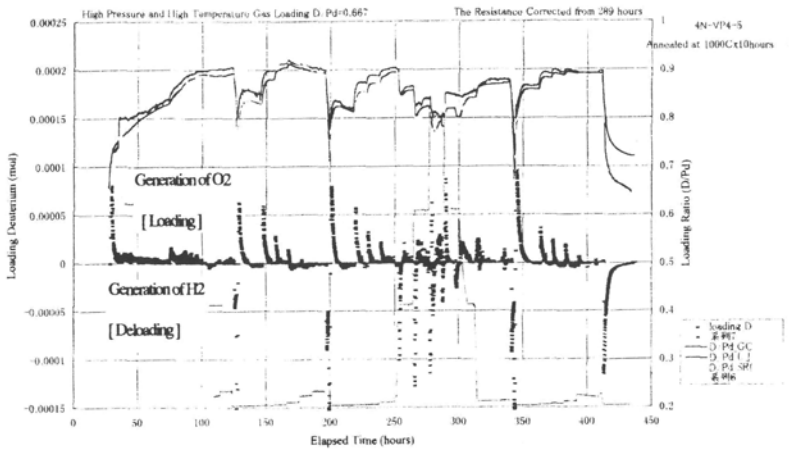

Fig.6 Deuterium loading into Pd measured by GC analysis

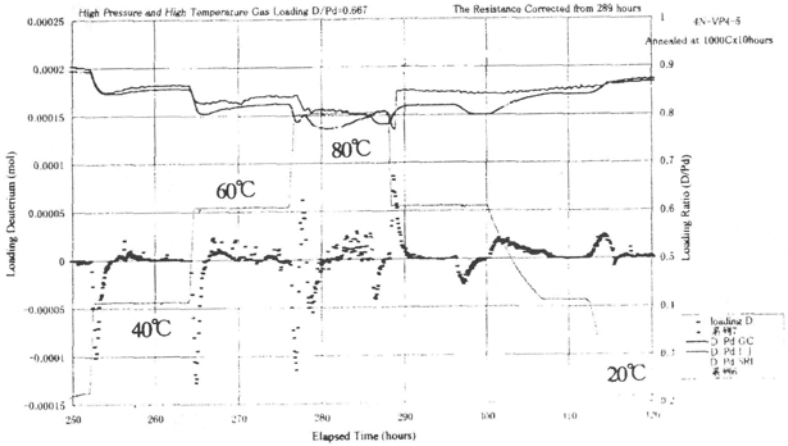

Fig.7 Temperature dependence on d-loading measured by GC analysis

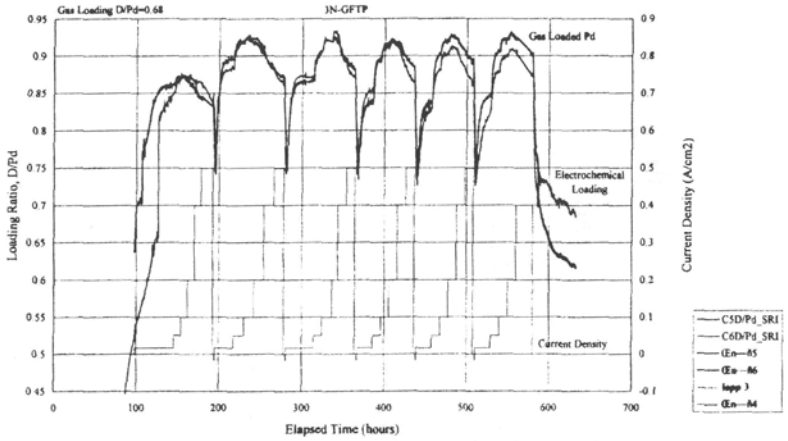

Fig.8 Loading curve for both samples, pre-loading by HT/HP gas and electrochemical loading only

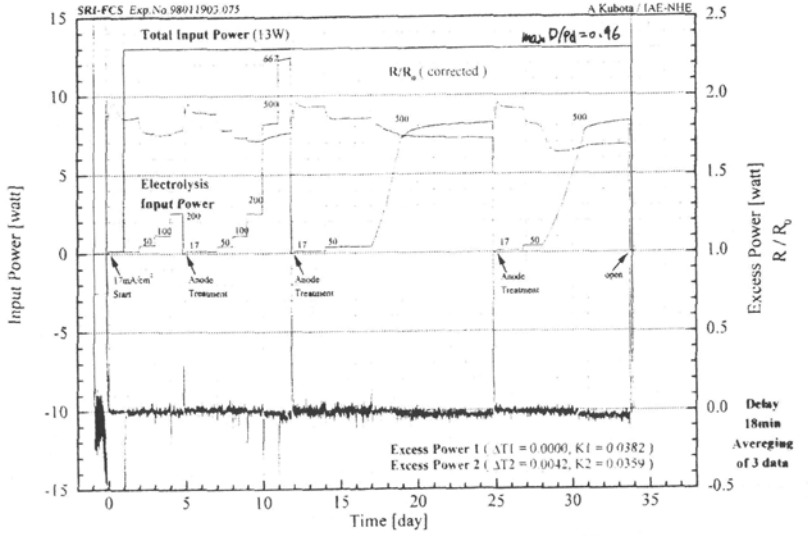

Input Power, Excess Power, R/R_0 v.s. Electrolysis Time

Fig.9 Excess heat measurement with HT/HP pre-loading specimen

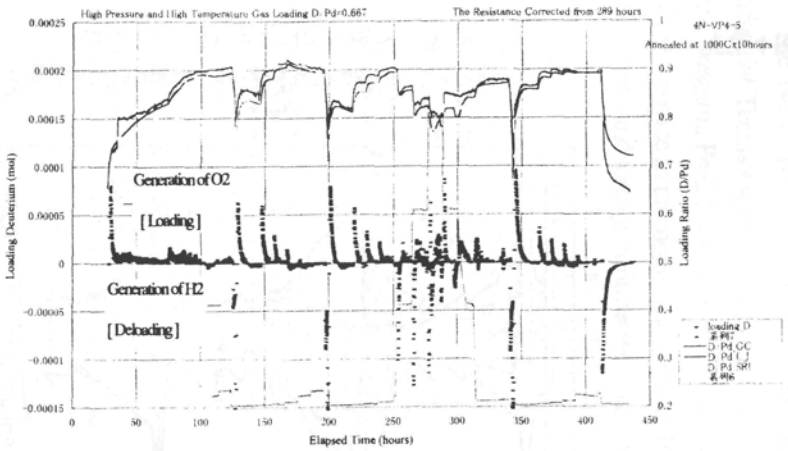

Fig.6 Deuterium loading into Pd measured by GC analysis

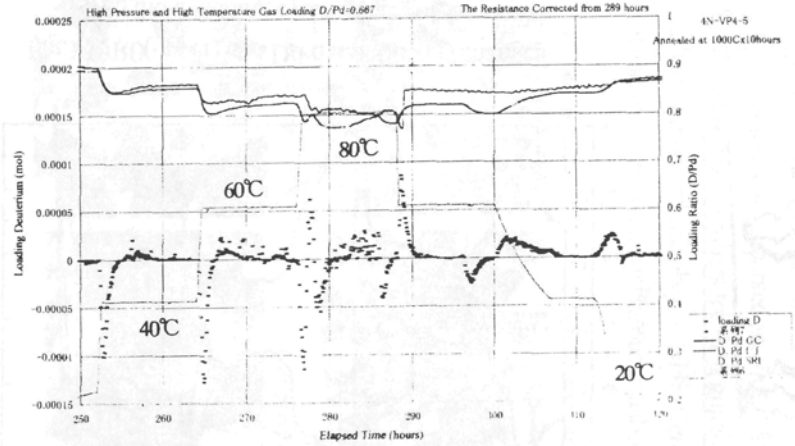

Fig.7 Temperature dependence on d-loading measured by GC analysis

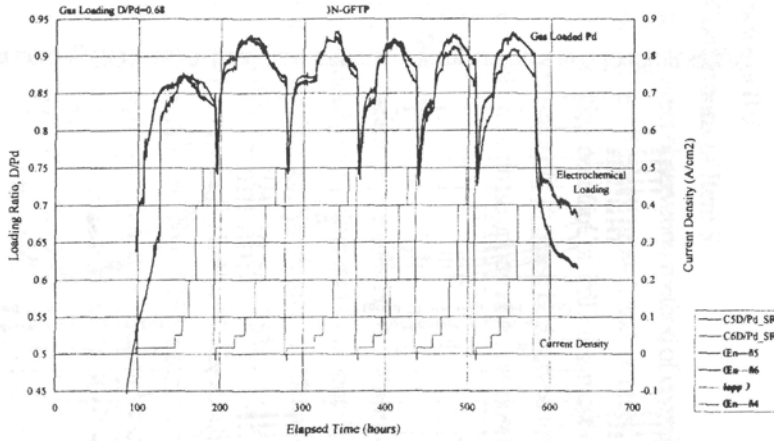

Fig.8 Loading curve for both samples, pre-loading by HT/HP gas and electrochemical loading only

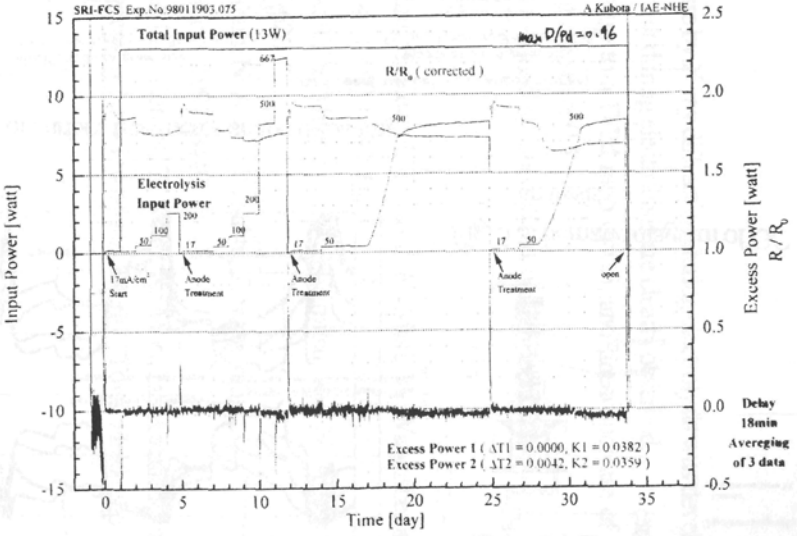

Input Power, Excess Power, R/R_0 v.s. Electrolysis Time

Fig.9 Excess heat measurement with HT/HP pre-loading specimen

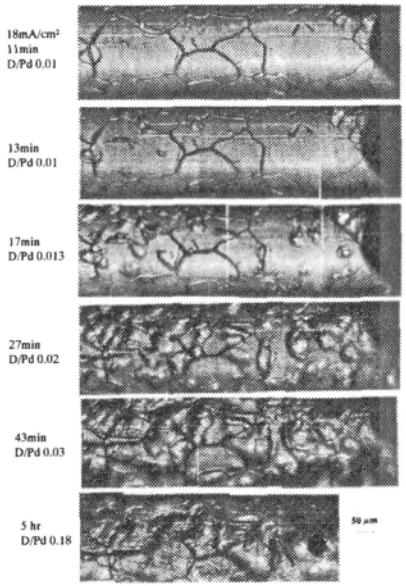

Photo-2 Growth of β phase and slip band formation during electrolysis on 4-nine heat treated Pd

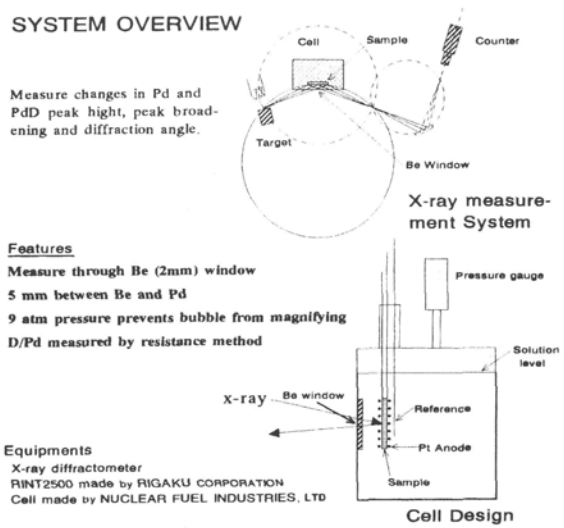

Fig.10 Schematic figure of in-situ X-ray diffraction system

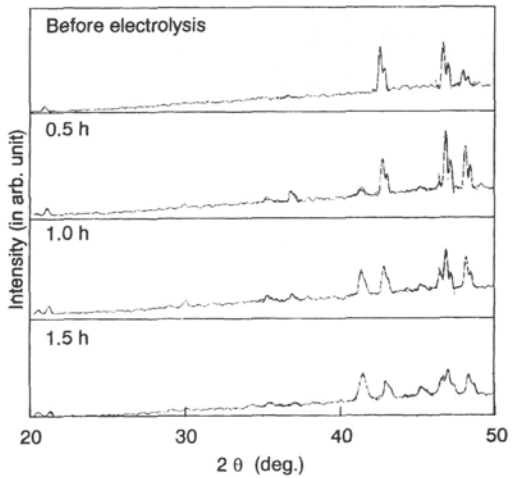

Fig.11 Examples of diffraction pattern for the initial stage of Pd electrolysis. β phase growth is observable.

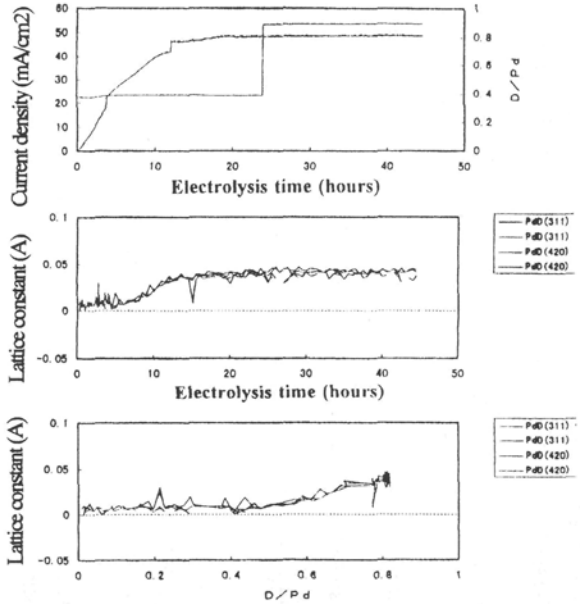

Fig.12 Lattice constant change of 4-nine Pd during electrolysis

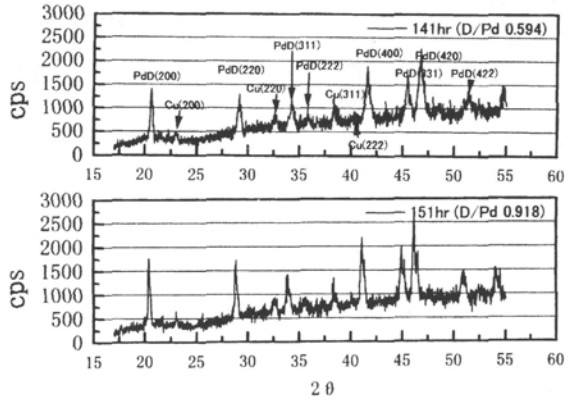

Fig.13 Diffraction patterns of deuterated Pd D/Pd at 0.59 (upper) and 0.92(lower)